International Journal of Signal Processing, Image Processing and Pattern Recognition
Vol.9, No.7 (2016), pp.93-106
http://dx.doi.org/10.14257/ijsip.2016.9.7.09

Face Contour Segmentation Based on Prior Information and Level Set Method

Ji Zhao[1], Huibin Wang[2] and Wenge Huang[3]

School of Software Engineering
University of Science and Technology Liaoning
Anshan, China
1zhaoji_1974@126.com

Abstract

The prior knowledge of face scale and shape are introduced into active contour model for face contour segmentation. Based on the variance of each column about image and the gradient of variance, the face outline size and central coordinates are obtained. The level set functions of the collected shapes are used as training data, which are projected onto a low dimension subspace. The attribute reduction of training set by PCA method is approximated Gaussian distribution. A constructed shape prior model with facial personality traits is incorporated into variational level set model based on boundary and region to constrain the contour evolution process, and then model can be accurately evolved into the face boundary. Experimental results validate the efficiency of this method.

Keywords*: Face segmentation, Shape prior, Level set, Variance, Gradient*

1. Introduction

Face segmentation is a hot topic in the field of image processing and the accurate segmentation of face contour, also it plays a key role in face recognition, analysis of facial expression and understanding of various emotions [1-2]. Many factors can influence face detection and segmentation, such as color, light conditions, changes and representation of the position, the distance between camera and the main body, *etc*. Face segmentation includes two steps: face positioning and the extraction of face boundary. Many methods proposed for face precise positioning. T.F. Cootes [3] *et al.* put forward the Active Shape Model (ASM) which utilizes as heuristic information the feature point of the local gray level texture features. Consequently, it not only easily falls into local minimum but also results the low accuracy of face positioning. G.J. Edwards [4] *et al.* put forward the Active Appearance Model (AAM) which integrates shape and texture information. Compared with the ASM, the AAM improves accuracy, but it may cause the failure of positioning if the initial position drifts away from face due to the sensitivity of the initial position of the model.

In order to solve face segmentation problems, many methods have been proposed at home and abroad. Féraud R [5] *et al.* put forward Neural network method; Wu H [6] put forward a fuzzy pattern matching method and Herodotou N [7] *et al.* proposed a new method based on color information and geometry knowledge. At home, Wu L.F. [8] proposed face segmentation algorithm on the basis of curve fitting. Although many scholars remain committed to the research of face segmentation, there is still no a definitive method which consider the various factors like light, shade, the complex background, and the location of facial contour.

In the past few years, the active contour model propounded by Kass M [9] has attracted great attention because of its comprehensive theoretical basis and better robustness. There are two broad categories in the current active contour model, the parametric active

ISSN: 2005-4254 IJSIP

contour model and the geometric active contour model [10]. The parametric model is characterized by its concise expression and quick implementation. But difficult to deal with separatist or fusion topology problems occur during deformation, the geometric model can handle natural topology changes. Therefore, this paper employs the geometric model these two methods used based on level set theory, the mathematical theory basis is partial differential equation (PDE) [11] and the process of solving the equation is the process of image segmentation.

Caselles [12] *et al* put forward the boundary-based active contour model which is called GAC model, but the model is susceptible to the influence of the local minimum so that it is more sensitive to noise. D. Mumford and J. Shah [13] proposed the region-based M-S model, it may lead to the inaccurate boundary positioning since it only utilizes region information. In order to overcome the defects of the above-mentioned two models, researchers have introduced some prior shape information to improve the robustness of the algorithm. Gastaud M [14] *et al*. combined shape prior and statistical features for active contour segmentation, which tracked and segmented face in video successfully. Cremers D [15] used dynamical statistical shape priors to solve the moving target segmentation. S. Y. Yeo [16] proposed a novel level set segmentation method by using the statistical prior shape of the variational method. J. Y. Dong [17] proposed priori shape segmentation model based on principal component analysis and maximum a posteriori. P. H. Lim [18] combined the prior shape and Willmore Flow to drive the level set evolve, and applied it to spinal CT image segmentation successfully.

Against the characteristics of face contour, this paper put forward a variational level set method based on region and edge which fuses face position, dimension and shape information. Additionally, constraint information has been merged into the energy function to improve the accuracy and robustness of the algorithm.

Based on the previous discussion, the basic concepts of this algorithm are as follows. First, determine the region and position of face to limit the search area of the face contour edge. Second, position the level set based evolution curve at the edge of face which is guided by image gradient, regional information and priori shape, and then face segmentation will be achieved.

2. The Novel Method Proposed in This Paper

This paper proposes a method to estimate the size of the face contour and the center coordinates. The method makes full use of the characteristics of gray value to get four borders around the image by calculating variance, gradient and other statistics. The proportion of width and height of the face conforms to a Gaussian distribution and face is considered as ellipse approximately, thus the area of face and center coordinates are calculated. Finally according to the area and center coordinates, we can acquire the scaling, translation amount and other segmentation parameters indirectly.

2.1. Left and Right Boundaries of Face

This paper assumes a coordinate system whose origin in the upper left corner of the image, and the positive direction of X-axis and Y-axis are rightward and downward. N , M represent width and height of the image, respectively. So the image area is $[0, N-1]\times[0, M-1]$. The present paper uses several statistics, which is defined by:

$$mean_j = \frac{1}{M}\sum_{i=1}^{M} x_i \tag{1}$$

$$v_j = \frac{1}{M}\sum_{i=1}^{M}(x_i - mean_j)^2 \tag{2}$$

$$g_j = \begin{cases} g_j = v_j & j = 1, N \\ g_{j+1} - g_{j-1} & j = 2, ..., N-1 \end{cases} \quad (3)$$

Where $mean_j, v_j, g_j$ denote respectively the mean, variance and gradient of the gray scale of the jth column in the image and i=1,…,M, j=1,…,N.

In a horizontal direction from left to right, according to the image gray variance and the change of gradient of each column, the image can be roughly divided into five or six parts in Figure1.

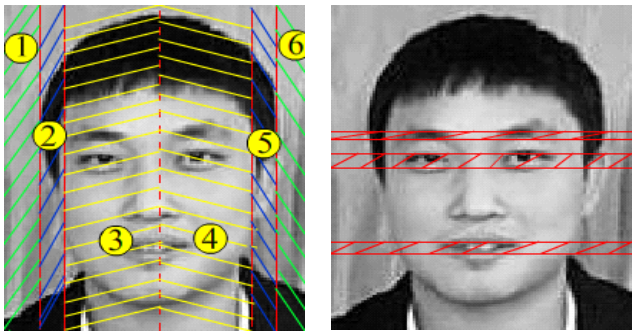

(a) (b)

Figure 1. (a)Face Division. (b)Interference Region of the Lower Boundary of Face

(1) Between the left boundary of the image and the left boundary of the head image, scilicet ①in Figure1(a), the change of the gray scale is basically stable. The gradient of gray variance changes a little, and it just goes up and down near 0, as shown ①in Figure 3.

(2) Between the left boundary of the head image and the left boundary of the facial image, scilicet ②in Figure1(a), the change of the gray scale increases sharply, and then slowly decreases slowly as shown ②in Figure2. The corresponding gradient also rises fast, then falls fast, and then begins to increase, as shown ②in Figure3. That is, gradient is responsive to the changing speed of variance. The greater the gradient is, the faster the variance changes.

(3) Between the left boundary of the facial image and the right boundary of the facial image, scilicet ③and ④in Figure1(a), because of the mixed gray scale of facial features, the cluttered change of the variance and the regular variations of the corresponding gradient are poor, as shown ③in Figure2.

(4) Between the right boundary of the facial image and the right boundary of the head image, scilicet ⑤in Figure1(a), the law of this part is similar to ②, but just in the reverse order.

(5) Between the right boundary of the head image and the right boundary of the image, scilicet ⑥in Figure1(a). The law of this part is similar to ①.

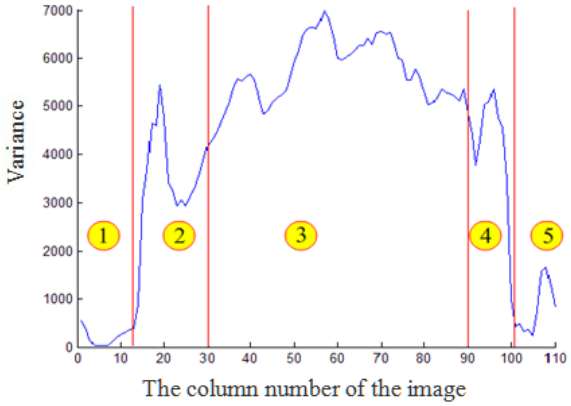

Figure 2. Variance Sequence of Image Column

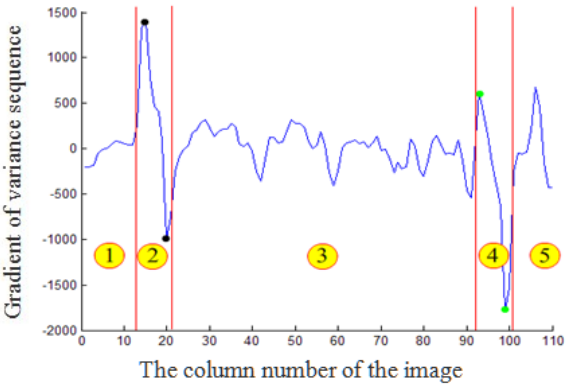

Figure 3. Gradient and Division of Variance Sequence

According to the distribution law of the image gray variance, the face of left and right boundaries can be calculated. Between ①and ②in Figure3, the corresponding gradient will have a maximal limit which is the far left boundary of the head image. Between ② and ③in Figure3, there is the second maximum value whose position is the actual location of the left boundary of the facial image. Similarly, there is a minimum value between ③and ④in Figure3 as well as between ④and ⑤in Figure3. The minimum is entirely caused by the calculation method of the gradient. The first minimum is the actual right boundary of the facial image while the second is the right boundary of the head image. The computational process from left to right boundaries of the facial image is as follows:

a. The gray-scale variance of each column of image is expressed as v_j calculates according to formula (1) and (2).

b. The gradient of v_j which is expressed as g_j calculates according to formula (3).

c. Finding the max value which is assumed g_m within $g_1, g_2 \cdots, g_k$ and looking for the first min value within $g_{m+1}, \cdots, g_k$, then the corresponding index number of achieved value is the left boundary of face which is expressed as la .

d. Finding min value which is assumed g_n within $g_N, g_{N-1} \cdots, g_P$ and looking for the first max value within $g_{n-1}, \cdots, g_P$, then the corresponding index number of achieved value is the right boundary of face which is expressed as ra .

The above four dots are marked with black dots and green dots in Figure3, respectively.

2.2. Upper and Lower Boundaries of Face

Similarly, we can calculate the image gray-scale variance of each row; and work out the upper boundary of face which is expressed as tb according to the gradient of above value. The characteristic of the image is the reason why we need to calculate the upper boundary instead of the lower boundary. As shown in Figure1 (b), due to the most of image is head , and that facial features are long and narrow strip in the X direction, the variance is more prominent and the gradient is more obvious in the row of these areas. Due to the differences of the clothes, the variance and gradient of the lower boundary is not obvious. The interferential areas mainly show in the face, eyebrows, eyes, nose, lips, *etc*. So the method is difficult to determine the lower boundary.

The ratio of height and width conforms to the Gaussian distribution whose average is about 1.33 and the variance is 0.0142, through recording almost 200 homogeneous face images. The range is within ±0.35 by 3σ standard of statistics. From the characteristics of variance, the volatility of ratio is low. Calculation is estimate value, so the value fully meets the requirements. The width of face can be gained by ra and la , as formula (4) shows. Width times 1.33 is the height of face, as formula (5) indicates. And tb plus the height is the under boundary of face.

$$width = ra - la \tag{4}$$

$$height = width \times 1.33 \tag{5}$$

2.3. The Area of Face and Center Coordinates

If face is regarded as an approximate ellipse, the width corresponds to short axis and the height corresponds to long axis. The calculation of the area of face is shown in formula (6). As for the center of face, the center of left and right boundaries of face can instead which is denoted x_0 . The half of the distance between the upper boundary and the lower boundary expresses y_0 . The computational formula of x_0 and y_0 is shown in formula (7).

$$S = \pi \times (width/2) \times (height/2) \tag{6}$$

$$\begin{cases} x_0 = (la + ra)/2 \\ y_0 = (tb + width)/2 \end{cases} \tag{7}$$

3. The Basic Concepts of Algorithm

3.1. Obtaining the Sample Sets

The present paper chooses the facial shapes which are segmented from the representative 18 face images as the initial training sample set, they are shown as follows.

Figure 4. Original Frontal Face

3.2. The Registration of the Shape Training Set

This experiment does binarization processing on each of the facial shapes and the specific steps of the registration includes: translation, rotation and scaling, where translation formula is defined by

$$x^k = \frac{\sum_{i=1}^{m}\sum_{j=1}^{n} x_i \chi_k(x_i, y_j)}{\sum_{i=1}^{m}\sum_{j=1}^{n} \chi_k(x_i, y_j)} \qquad y^k = \frac{\sum_{i=1}^{m}\sum_{j=1}^{n} x_i \chi_k(x_i, y_j)}{\sum_{i=1}^{m}\sum_{j=1}^{n} \chi_k(x_i, y_j)} \tag{8}$$

Where $k = 1, 2, ..., 18$, m and n respectively denote the number of rows and columns in a binary image, (x_i, y_i) represents the coordinate which corresponds to the pixels in a binary image. χ_k denotes the kth binary image. After calculating barycentric coordinate of each sample binary image, we can solve the relevant translation volume which responds to each referred image. The scaling formula is defined by

$$s^k = \frac{1}{L^k}\sum_{i=1}^{L^k} d\left(\left(x_i^k, y_i^k\right), \left(x^k, y^k\right)\right) \tag{9}$$

Where $d\left(\left(x_i^k, y_i^k\right), \left(x^k, y^k\right)\right)$ denotes the Euclidean distance between the coordinate $\left(x_i^k, y_i^k\right)$ on the edge of the target contour and the barycentric coordinate (x^k, y^k). So the zoom scale of the kth sample binary image can be defined by s^k / s^l, where s^l is the average distance between point on the contour edge of the chosen referred binary image and the barycentric coordinate of the image.

The final sample training set after translation, scaling and rotation is shown in Figure5.

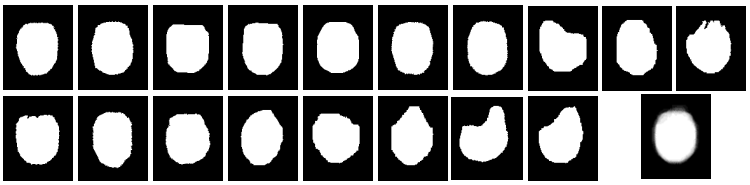

Figure 5. Face Contour Pan, Zoom and Rotation Mages

3.3. The Level Set Expression of the Training Sample

It is necessary to use formula of SDF to calculate the SDFs which correspond to the training sample shapes shown in Figure6 and level set representation of the SDFs of each training sample are shown in Figure6. In Figure6, the closed line denotes the contour line

of each training samples shown in Figure6, So far, we obtain the zero level set of all the training samples, which are defined by $\phi_1, \phi_2, ..., \phi_{18}$.

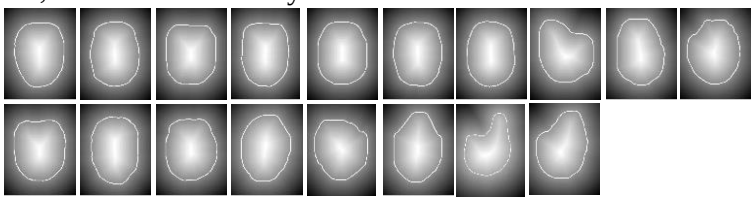

Figure 6. Level Set Representation of Training Samples

3.4. Using PAC to Establish a Prior Shape Model

In order to reduce the redundant information, Leventon applied the PCA method to calculate the SDF of the contour, and improved registration process in some respects which are robustness, accuracy and speed. So the ideal segmentation results can be obtained. This paper adopts the method which is similar to Leventon M E[19]. In algorithm implementation process, the degree of fitting adopted in the experiment is p=0.98. When the cumulative contribution rate of the first t eigenvalues is equal to or greater than 0.98, the first t eigenvalues and the corresponding eigenvectors are chosen as principal components which denote the new sample shape. After decreasing dimensions of the SDFs by PCA method, k meeting the requirements is equal to 9. In this way, the original 18 SDFs of the samples are replaced by the reconstructed 9 SDFs of the samples which are used as a new sample prior shape.

The last step of PCA is the reconstruction of the data; the new SDF is gained by formula (10).

$$\hat{\phi} = \mathrm{E}_k \mathbf{x}_{\mathrm{pca}} + \bar{\phi} \tag{10}$$

Where characteristic coefficient x_{pca} is the weight coefficient which has k patterns of change. Apparently the sample average image can be got when x_{pca} is zero vector.

Figure 7 shows the average image and 9 images which use main model reconstructions separately. In subgraph (1) ~ (9), the left-hand image is using $2\sqrt{\lambda_i}$ serve as characteristic coefficient while the right-hand image is using $-2\sqrt{\lambda_i}$ serve as characteristic coefficient. They all change within their own space on the basis of the average image.

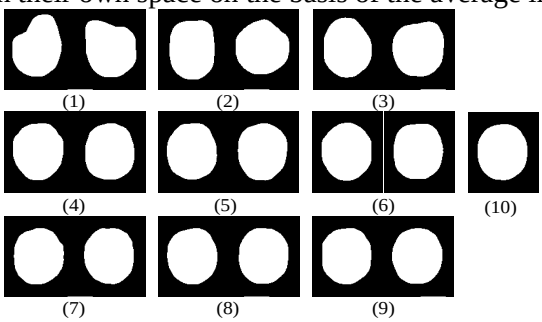

Figure 7. Graphics Reconstruction by the Main Mode

As shown in Figure7, the changes of subgraph are less obvious from (1) ~ (9). Moreover, there are few changes in subgraph (4) ~ (9). The proportion of eigenvalue in each model can see analogue. Through calculating, the proportion of each eigenvalue is

P= {0.5595, 0.2174, 0.1167, 0.0355, 0.0233, 0.0202, 0.0158, 0.0063, 0.005} , and the fitting of the first three characteristic patterns of degree is 0.8932.

4. Level Set Method Based on Prior Information

4.1. Prior Scale Information

First, the boundary location of the facial position can be automatically obtained before segmentation, then we calculate the area of the face and center coordinates. The mean area of prior shape divided by the area which gets by this method is scaled estimated value S . Besides that, the center of mean image of prior shape minus the center which estimates by present method is translation vector. The calculation formulas are shown as follows:

$$S = S_m / S_0 \tag{10}$$

$$T(x,y) = \begin{cases} x = x_m - x_0 \\ y = y_m - y_0 \end{cases} \tag{11}$$

Where S_m is mean area of prior shape, x_m denotes center of the X coordinate and y_m stands for center of the Y coordinate, and S_0, x_0, y_0 respective denote mean area of prior shape, center of the X coordinate and center of the Y coordinate which by present method.

4.2. Level Set Model Based on Prior Shape

Segmentation method in this paper is a combination of shape priori information, edge information and regional information. The energy functional is as follows:

$$F = \beta_s F_{shape}(C, \mathrm{x}_{pca}, \mathrm{x}_T) + \beta_b F_{boundary} + \beta_r F_{region}(\mathrm{x}_{pca}, \mathrm{x}_T, u_{in}, u_{out}) \tag{12}$$

Where

$$F_{shape} = \oint_0^1 \hat{\phi}\left(\mathrm{x}_{pca}, h_{XT}(C(q))\right)\left|C'(q)\right|dq \tag{13}$$

$$F_{boundary} = \oint_0^1 g(\left|\nabla I(C(q))\right|)\left|C'(q)\right|dq \tag{14}$$

$$F_{region} = \int_{\Omega_{in}(\mathrm{x}_{pca},\mathrm{x}_T)} (\left|I - u_{in}\right|^2 + \mu\left|\nabla u_{in}\right|^2 d\Omega) + \int_{\Omega_{out}(\mathrm{x}_{pca},\mathrm{x}_t)} (\left|I - u_{out}\right|^2 + \mu\left|\nabla u_{out}\right|^2 d\Omega) \tag{15}$$

Where C is active contour, ϕ is interested target shape function given by PCA, x_{pca} is the vector of characteristic coefficient of PCA, h_{XT} is a set of elements of geometric transformation parameterized by x_T . g is a edge function, Ω_{in} and Ω_{out} are internal and external region of zero level set ϕ, u_{in} and u_{out} are flat approximate of the original image I within Ω_{in} and Ω_{out} . $\beta_b, \beta_s, \beta_r$ are arbitrary positive constants, which are used to balance the contributions of boundary, shape and area respectively. ϕ denotes the zero level set function, we can use the level set framework to represent the functional F which is as follows:

$$F = \int_\Omega f\left(x, \mathrm{x}_{pca}, \mathrm{x}_T\right)\left|\nabla\varphi\right|\delta(\varphi)d\Omega + \beta_r \int_\Omega \left(\Theta_{in} H\left(\hat{\phi}\left(\mathrm{x}_{pca}, \mathrm{x}_T\right)\right) + \Theta_{out} H\left(-\hat{\phi}\right)\right)d\Omega \tag{16}$$

Where

$$f\left(x, \mathrm{x}_{pca}, \mathrm{x}_T\right) = \beta_s \hat{\phi}^2\left(\mathrm{x}_{pca}, h_{\mathrm{x}_T}(x)\right) + \beta_b g\left(\left|\nabla I(x)\right|\right) \tag{17}$$

$$\begin{aligned} \Theta_{in} &= \left|I - u_{in}\right|^2 + \mu\left|\nabla u_{in}\right|^2 \\ \Theta_{out} &= \left|I - u_{out}\right|^2 + \mu\left|\nabla u_{out}\right|^2 \end{aligned} \tag{18}$$

Where $H(\bullet)$ is often replaced by regularized Heaviside Function which is defined by:

$$H_\varepsilon(x) = \frac{1}{2}\left(1 + \frac{2}{\pi}\arctan\frac{\pi x}{\varepsilon}\right) \tag{19}$$

The derivative of H_ε is defined as follows, which is called as $\delta_\varepsilon(x)$

$$\delta_\varepsilon(x) = H_\varepsilon^{'}(x) = \frac{1}{\pi}\frac{\varepsilon}{\varepsilon^2 + x^2} \tag{20}$$

Where ε is regularization parameter and it is 1.5 in the experiment. Formula (21) is revised as follows:

$$F = \int_\Omega f\left(x, \mathrm{x}_{pca}, \mathrm{x}_T\right)\left|\nabla\varphi\right|\delta_\varepsilon(\varphi)d\Omega + \beta_r\int_\Omega\left(\Theta_{in}H_\varepsilon\left(\hat{\phi}\left(\mathrm{x}_{pca}, \mathrm{x}_T\right)\right) + \Theta_{out}H_\varepsilon\left(-\hat{\phi}\right)\right)d\Omega \tag{21}$$

The evolution equation of minimizing the functional F is as follows:

$$\begin{cases} \partial_t\varphi(t,x) = \left(f\kappa - \left\langle\nabla f, \dfrac{\nabla\varphi}{|\nabla\varphi|}\right\rangle\right)\delta_\varepsilon(\varphi) \;\; in\;[0,\infty]\times\Omega \\ \varphi(0,x) = \varphi_0(x) \;\; in\;\Omega \\ \dfrac{\delta_\varepsilon\varphi}{|\nabla\varphi|}\partial_N\varphi = 0 \quad on\;\partial\Omega \end{cases}$$

$$\begin{cases} d_t\mathrm{x}_{pca}(t) = -\int_\Omega \nabla_{\mathrm{x}_{pca}}\hat{\phi}\left(2\beta_s\hat{\phi}\left|\nabla\varphi\right|\delta_\varepsilon(\varphi)\right. \\ \qquad \left. + \beta_r(\Theta_{in} - \Theta_{out})\delta_\varepsilon\left(\hat{\phi}\right)\right)d\Omega \;\; in[0,\infty]\times\Omega_{pca} \\ \mathrm{x}_{pca}(t=0) = \mathrm{x}_{pca_0} \quad in\;\;\Omega_{pca} \end{cases}$$

$$\begin{cases} d_t\mathrm{x}_T = -\int_\Omega\left\langle\nabla\hat{\phi}, \nabla_{\mathrm{x}_T}h_{\mathrm{x}_T}\right\rangle\left(2\beta_s\hat{\phi}\left|\nabla\varphi\right|\delta_\varepsilon(\varphi)\right. \\ \qquad \left. + \beta_r(\Theta_{in} - \Theta_{out})\delta_\varepsilon\left(\hat{\phi}\right)\right)d\Omega \;\; in[0,\infty]\times\Omega_T \\ \mathrm{x}_T(t=0) = \mathrm{x}_{T_0} \quad in\Omega_T \end{cases}$$

$$\begin{cases} \partial_t u_{in}(t,x) = u_{in} - I - \mu\Delta u_{in} \quad in[0,\infty]\times\left\{\hat{\phi} > 0\right\} \\ u_{in}(0,x) = I \;\; in\left\{\hat{\phi} > 0\right\} \\ \partial_t u_{out}(t,x) = u_{out} - I - \mu\Delta u_{out} \quad in[0,\infty]\times\left\{\hat{\phi} < 0\right\} \\ u_{out}(0,x) = I \;\; in\left\{\hat{\phi} < 0\right\} \end{cases}$$

Where $\mathrm{x}_T = (s,\theta,T)$, s, θ, T denote scaling factors, rotation factors and translation amount respectively.

5. Experimental Results and Analysis

5.1. Experimental Results

Figure8 is the segmentation result of the ten 110×140 front face image which adopts fixed default initial parameter, where scaling factor is 1, rotation factor is 0 and translation amount $T=(0,0)$.

It can be seen from Figure9 that the proposed method segments the facial contour almost correctly.

Figure 8. The Results with Default Parameters

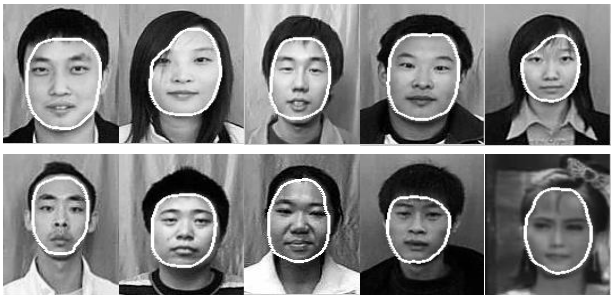

Figure 9. The Results of the Proposed Method

The actual value, experimental value and its error of the area and the center coordinates of the face are shown in Table1 and in Table2.

Table 1. Area of Face

Number	*1*	*2*	*3*	*4*	*5*	*6*	*7*	*8*	*9*	*10*
Actual value	*5206*	*4711*	*3592*	*4460*	*2933*	*3360*	*3269*	*3283*	*2844*	*3820*
Experimental	*5700*	*5387*	*3326*	*4434*	*3266*	*2916*	*3610*	*3088*	*3448*	*3699*
Value error	*494*	*676*	*266*	*26*	*333*	*444*	*241*	*195*	*604*	*121*

Using 3σ standard can gain that the range of area is ± 632.4 and the range of x, y coordinates is ± 5.03 and ± 13.8. Most errors of facial area are within 500 and center coordinates are within 10.The previous errors are tolerated through the actual segmentation effect.

The parameters of formula (18) and formula (24) are shown in Table 3.

The corresponding scale parameters of all image are {1.051, 1.112, 1.3012, 1.2012, 1.3344, 1.4543, 1.2868, 1.3997, 1.3174, 1.2697}, and the initial translation amount are {(-4.5795,-21.421),(-5.0795,-5.0212),(-0.5795,-7.5212),(-5.3295,-8.4712),(-5.8295,1.8288),(-3.3295,10.929),(-8.3295,-15.571),(-3.5795,0.8788),(-1.5795,-7.2212),(-13.58,2.3788)}.

From Figure10 we can see that the method proposed by this paper is feasible. Although parameters gained by this method are not correct completely, their errors almost do not affect the segmentation method.

Table 2. The Center Coordinates of the Face

Number	*1*	*2*	*3*	*4*	*5*	*6*	*7*	*8*	*9*	*10*
Actual value	*56.7*	*62.09*	*50.67*	*56.63*	*60.15*	*54.91*	*59.16*	*50.65*	*51.71*	*66.40*
	80.06	*71.62*	*77.29*	*73.19*	*58.44*	*54.10*	*77.39*	*60.92*	*76.16*	*81.84*
Experimental	*57*	*57.5*	*53*	*57.75*	*58.25*	*55.75*	*60.75*	*56*	*54*	*66*
	89.4	*73*	*75.5*	*76.45*	*66.15*	*57.05*	*83.55*	*67.1*	*75.2*	*65.6*
Value error	*0.3*	*4.49*	*2.33*	*1.12*	*1.9*	*0.84*	*1.59*	*5.35*	*2.29*	*0.4*
	8.8	*1.83*	*1.79*	*3.26*	*7.71*	*2.95*	*6.16*	*6.18*	*0.96*	*16.24*

Table 3. Parameter Setting

Parameter	*βb*	*βs*	*βr*	*μ*
Value	*1*	*0.5*	*100*	*50*

In Figure10 from left to right, the first column denotes the original images, the second column denotes segmentation results by the C-V method[20], the third column denotes segmentation results by GAC, and the last column segmentation results from the previous method.

In the first row, Figure10 (a) is a 110×140 grayscale image and we can see that the C-V method is able to segment other regions within the active contour. The segmentation speed of the GAC method is slower than that of the C-V method, and edge leakage phenomenon may occur because the fuzzy boundaries.

In this method we set the scaling equal to 1.1023 and the translation amount is (-5.5374,-5.5132), and the effect of face segmentation is ideal. Even if it goes on iterating, the shape of the active contour is remained stable for this approach basically.

In the second row, Figure10 (a) adds the obstacle factitiously which is beyond the scope of face. Figure10 (b) is a segmentation result which utilizes the C-V method through iterating 100 times. Figure10 (c) is a segmentation result which utilizes the GAC method through iterating 2800 times. Figure10 (d) is a segmentation result which utilizes the present method through iterating 1200 times. We can see that segmentation result of this method is ideal. Although under the interference of obstacles, it can still segment the facial contour correctly.

In the third row, Figure10 (a) is a front face image that wears a mask; if the C-V method iterates 100 times, the GAC method iterates 2100 times. The scaling is 1.0783 and the translation amount is (-3.5795,-20.621) when use the present method. As can be seen from the segmentation results, obstacle and face are divided into two regions for the C-V method and the GAC method, while segmentation method described in this paper meets the requirements of the face segmentation basically.

In the last row, Figure10 (a) is a facial fuzzy image. The C-V method iterates 100 times, the GAC method iterates 2100 times and the novel method iterates 480 times. The scaling is 1.2652, and the amount which obtained automatically and translation are (-6.5795,-27.321).So we can see that this method has good robustness for fuzzy image segmentation.

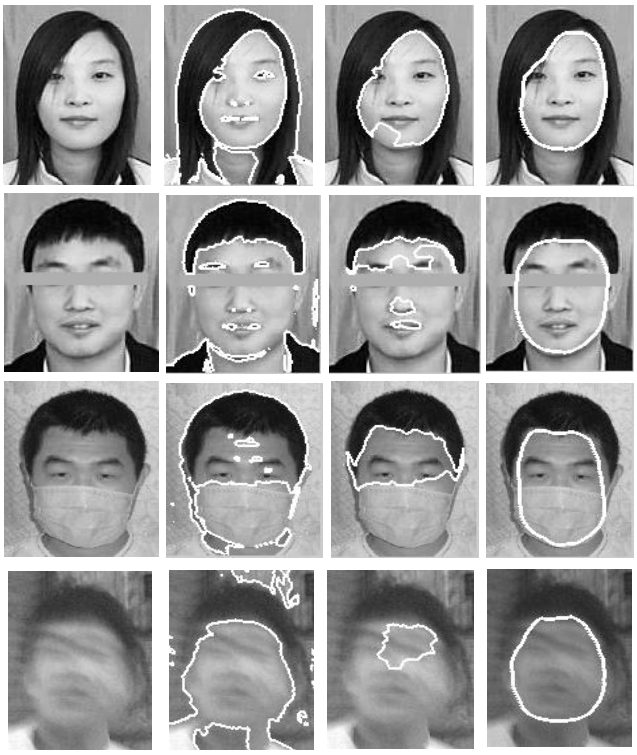

Figure 10. (a)Original Image (b)C-V Method (c)GAC Method (d)The Proposed Method

5.2. Experimental Analysis

The paper adopts misclassification error as the evaluation algorithm of experiment results, and the formula is shown as follows:

$$ME = \frac{Area\{S_A \cup S_B\} - Area\{S_A \cap S_B\}}{Area\{S_B\}} \tag{22}$$

Where we set S_A to segmentation contours and set S_B to object contours. The smaller ME is, the better segmentation result is. Algorithm segmentation result is consistent with the manual segmentation result when ME is 0.

Table 4. The MEs for the Different Methods

Method	*Mean ME*
C-V	*17.3912*
GAC	*6.4136*
Our method	*0.3215*

The contrast of misclassification error of 200 front face image segmentation results using three above-mentioned algorithms is shown in Table4. Experiments show that segmentation effects of the C-V method and the GAC method are not ideal, two mean ME are 17.3912 and 6.4136, respectively. But the method in this paper can gain better segmentation results and the mean ME is 0.3215 which is smaller than that of the method of C-V and GAC.

6. Conclusion

The present paper puts forward the method which can compute the image face boundary through in-depth analysis of the image characteristics. Theoretical analysis and experimental results prove that the method is effective and workable. It can avoid factitiously set parameters and increase the adaptability of image segmentation. In the level set segmentation model based on edge and region, statistical prior shapes are introduced to improve the robustness of the segmentation. In addition, the complexity of the algorithm operation is improved due to prior shape. Future research will focus on the cases which have few differences between the brightness of background and foreground, and we are still able to segment effectively and precisely.

Acknowledgements

This Research is funded by the Education Department of Liaoning Province Foundation grant Number LJQ2014033 and University of Science and Technology Liaoning Foundation grant Number 2013RC08.

References

[1] C. H. Xu, S. Li and T. H. Tan, "Automatic 3d Face Recognition From Depth and Intensity Gabor Features", Pattern recognition, vol. 42, no. 9, **(2009)**, pp. 1895-1905.
[2] X. GONG, G. Y. WANG, T. R. LI, X.-X. LI, R. XIA and L. FENG, "Face Segmentation Based on A Hybrid Energy Based Active Contour Model", Journal of Software, vol. 23, no. 4, **(2013)**, pp. 623- 638.
[3] T. F. Cootes, C. J. Taylor and D. H. Cooper "Active shape models-their training and application", Computer Vision and Image Understanding, vol. 61, no. 1, **(1995)**, pp. 38-59.
[4] G. J. Edwards, T. F. Cootes and C. J. Taylor, "Interpreting Face Images Using Active Appearance Models", In: Proceedings of 3rd International Conference on AFGR. Nara, JAPAN, **(1998)**, pp. 300-305.
[5] R. Feraud, O. J. Bernier and J. E. Viallet, "A Fast and Accurate Face Detection Based on Neural Network", IEEE Transactions Pattern Analysis and Machine Intelligence, vol. 23, no. 1, **(2001)**, pp. 42-53.
[6] H. Wu, Q. Chen and M. Yachida, "Face Detection from Color Images using a Fuzzy pattern Matching Method", IEEE Transactions Pattern Analysis and Machine Intelligence, vol. 21, no. 6, **(1999)**, pp. 557-563.
[7] N. Herodotou, K. N. Plataniotis and A. N. Venetsanopoulos, "Automatic Location and Tracking of the Facial Region in Color Video Sequences", Signal Process: Image Communication, vol. 14, no. 5, **(1999)**, pp. 359-388.
[8] L. F. Wu, L. S. Shen, X. Kong and X. J. Zhu, "Face Segmentation Based on Curve Fitting", Chinese Journal of Computers, vol. 26, no. 7, **(2003)**, pp. 893-897.
[9] M. Kass, A. Witkin and D. Terzopolos, "Snakes: Active contour model", International Journal of Computer Vision, vol. 1, no. 4, **(1987)**, pp. 321-331.
[10] C. Y. Xu and J. L. Prince, "Snakes, Shapes, and Gradient Vector Flow", IEEE Transactions Image Processing, **(1998)**, pp. 359-369.
[11] S. Osher and J. A. Sethian, "Fronts Propagating with Curvature dependent Speed: Algorithms based on Hamilton-Jacobi Formulations", Journal of Computational Physics, vol. 79, no. 1, **(1998)**, pp. 12-49.
[12] V. Caselles, R. Kimmel and G. Sapiro, "Geodesic active contours", International Journal of Computer Vision, vol. 22, no.1, **(1997)**, pp. 61-79.
[13] D. Mumford and J. Shah, "Optimal Approximations by Piecewise Smooth Functions and Associated Variational Problems", Commun. Pure Appl. Math., vol. 42, **(1989)**, pp. 577–685.
[14] M. Gastaud, M. Barlaud, G. Aubert, "Combining Shape Prior and Statistical Features for Active Contour Segmentation", IEEE Transactions on Circuits and Systems for Video Technology, vol. 14, no. 5, **(2004)**, pp. 726-734.
[15] D. Cremers, "Dynamical Statistical Shape Priors for Level Set Based Tracking", IEEE Transactions on Pattern Analysis and Machine Intelligence, vol. 28, no. 8, **(2006)**, pp. 1262 – 1273.
[16] S. Y. Yeo, X. Xie and I. Sazonov, "Level Set Segmentation with Robust Image Gradient Energy and Statistical Shape Prior", IEEE International Conference on Image Processing, Brussels, **(2011)**, pp. 3397-3400.
[17] J. Y. Dong and C. Y Hao, "Review of Statistical Shape Prior-based Level Set Image Segmentation", Computer Science, vol. 37, no. 1, **(2010)** January, pp. 6-9.
[18] P. H. Lim, U. Bagci and O. Aras, "A novel spinal vertebrae segmentation framework combining geometric flow and shape prior with level set method", IEEE International Symposium on Biomedical Imaging, Barcelona, **(2012)**, pp.1703-1706.

[19] M. E. Leventon, W. E. L. Grimson and O. Faugeras, "Statistical Shape Influence in Geodesic Active Contours", In: Proceeding of the IEEE Computer Society Conference on Computer Vision and Pattern Recognition, Los Alamitis, CA, USA, IEEE Computer Society, vol. 1, **(2000)**, pp. 316-323.
[20] T. Chan and L. Vese, " Active Contours without Edges", IEEE Transactions on Image Processing, vol. 10, no. 2, **(2001)** Febuary, pp. 266–277.

Authors

Ji Zhao is a professor in School of Software Engineering, University of science and technology Liaoning. He received the master degree in computer application technology in 2004 and Ph.D. degree in detection technology and automation equipment in 2013, both from Northeastern University China. His research interests include image segmentation and embedded technology and application. His present interests are expanded to face's localization, segmentation and expression understanding. He was a Visiting Researcher at Saitama University of industry, Japan in 2012.He was awarded the Liaoning Province Natural Science Academic Achievement prize from Liaoning science and Technology Association of China and Anshan Natural Science Academic Achievement prize from Anshan science and Technology Association of China in 2012.

